NATIONAL ADVISORY COMMITTEE FOR AERONAUTICS

TECHNICAL MEMORANDUM

No. 1095

WIND-TUNNEL INVESTIGATION OF THE HORIZONTAL MOTION OF A WING NEAR THE GROUND

By Y. M. Serebrisky and S. A. Biachuev

Central Aero-Hydrodynamical Institute

Washington
September 1946

NATIONAL ADVISORY COMMITTEE FOR AERONAUTICS

TECHNICAL MEMORANDUM NO. 1095

WIND-TUNNEL INVESTIGATION OF THE HORIZONTAL MOTION OF A WING NEAR THE GROUND[1]

By Y. M. Serebrisky and S. A. Biachuev

By the method of images the horizontal steady motion of a wing at small heights above the ground was investigated in the wind tunnel. A rectangular wing with Clark Y-H profile was tested with and without flaps. The distance from the trailing edge of the wing to the ground was varied within the limits $0.75 \leq \frac{s}{c} \leq 0.25$. Measurements were made of the lift, the drag, the pitching moment, and the pressure distribution at one section. For a wing without flaps and one with flaps a considerable decrease in the lift force and a drop in the drag was obtained at angles of attack below stalling. The flow separation near the ground occurs at smaller angles of attack than is the case for a great height above the ground. At horizontal steady flight for practical values of the height above the ground the maximum lift coefficient for the wing without flaps changes little, but markedly decreases for the wing with flaps. Analysis of these phenomena involves the investigation of the pressure distribution. The pressure distribution curves showed that the changes occurring near the ground are not equivalent to a change in the angle of attack. At the lower surface of the section a very strong increase in the pressures is observed. The pressure changes on the upper surface at angles of attack below stalling are insignificant and lead mainly to an increase in the unfavorable pressure gradient, resulting in the earlier occurrence of separation. For a wing with flaps at large angles of attack for distances from the trailing edge of the flap to the ground less than 0.5 chord, the flow between the wing and the ground is retarded so greatly that the pressure coefficient at the lower surface of the section is very near its limiting value ($\overline{p} = 1$), and any further possibility of increase in the pressure is very small. In the application an approximate computation procedure is given of the change of certain aerodynamic characteristics for horizontal steady flight near the ground.

---

[1]Report No. 437, of the Central Aero-Hydrodynamical Institute, Moscow, 1939.

INTRODUCTION

During recent years many papers have appeared which are devoted to the study of the ground effect on the aerodynamic characteristics of the airplane. The subject is of special interest because of its bearing on one of the most important problems of aerodynamics; namely, the landing and the take-off of an airplane. The main body of the investigations is concerned with the study of the horizontal steady motion near the ground. Such study cannot, of course, provide an answer to all questions arising in the solution of the above-mentioned problem. While, for example, for computing the magnitude of the induced drag in take-off it is still possible to use the scheme of horizontal steady flight near the ground this simplified scheme cannot be used in determining the landing speed, since there is the additional effect of rotational motion of the airplane that leads to the start of flow separation and unsteady flow as the airplane nears the ground. Both these factors result in an increase in the lift coefficient in landing. (See references 1 and 2.)

Together with the investigation being conducted at present of the unsteady parts of the landing path of the airplane, it was decided to supplement the existing data on the horizontal steady motion of a wing near the ground by an investigation of the case of small heights above the ground for wings with and without flaps. It was necessary also to clarify the question as regards the increase in the maximum lift coefficient for horizontal steady flight near the ground. The opinion exists that in the case of horizontal flight parallel to the ground where the heights above the ground are very small, a considerable increase in the lift force occurs at all angles of attack. As the present investigation has shown, however, a considerable increase in the maximum lift does not occur even when the height above the ground is small, although at small angles of attack the lift increases very appreciably. For the case of the wing with flaps at all heights from the ground there is a decrease in the maximum lift. It must again be emphasized that the writer is concerned with horizontal steady motion near the ground and not with landing, for which the greatest change is undergone by the portion of the polar curve near the maximum lift coefficient due to the start of the separation process.

The tests were conducted by the "method of images" on a model of a rectangular wing (with and without flaps). For

this wing together with the measurement of lift, drag, and moment of longitudinal stability the pressure distribution over the wing section near the ground also was found. Analysis of the pressure distribution curves explains the causes of the change in aerodynamic characteristics of the wing at horizontal steady flight near the ground.

NOTATION

α	angle of attack of wing
α_0	angle of attack corresponding to zero lift
c	wing chord
b	wing span
$\bar{h}$	ratio of maximum thickness of profile to chord
λ	aspect ratio of wing
δ_f	angle of deflection of flap
v	velocity of undisturbed flow in wind tunnel or flight velocity of airplane
ρ	mass density of air
x	distance along chord from leading edge
a_0	tangent of angle of inclination of lift curve for a wing of infinite span
$\bar{p}$	nondimensional pressure coefficient
H	distance from the axis of bound vertex of wing to ground
s	distance from trailing edge of wing to ground
s_1	distance from trailing edge of flap to ground
C_z	local normal force coefficient
$C_{z\,l}$	local normal force coefficient for lower surface of profile

c_{zu} local normal force coefficient for upper surface of profile

α_{lw} angle of attack of lower wing

α_{uw} angle of attack of upper wing

TEST PROCEDURE

In the CAHI T-5 wind tunnel having an open-work section and a diameter of the jet at the work section of 2.06 millimeters tests were conducted by the method of images on a model of a rectangular wing. Two identical wing models 1000 by 200 millimeters were prepared. A Clark Y-H profile with relative thickness h = 0.12 was chosen. One of the models (the lower one) was suspended on a six-component balance, the other (the upper) was not connected with the suspension system. The upper wing was located with respect to the lower wing as required by the method of images, that is, such that the upper and lower wings formed a symmetrical system with respect to a center plane passing between them corresponding to the plane on the ground. For the test a special setup was used that had been previously applied in the investigation of the case of great height above the ground. (See reference 3.) The lower wing was displaced downward from the tunnel axis by 150 millimeters. The angle of attack of the upper wing was controlled by an optical goniometer. During the test the distance between the trailing edges of the upper and lower wings was maintained constant while the angles of attack were varied. The tests were conducted for six different distances between the trailing edges (table I):

TABLE 1

2s (mm)	300	200	100	50	25	10
$\frac{s}{c}$	0.75	0.50	0.25	0.125	0.0623	0.025

Further, to the wings were also attached zap flaps, having a chord 30 percent of the wing chord and a 60° angle of flap deflection. In the tests with the flaps the distance ($2s_1$) between the trailing edges of the open flaps was maintained constant. Five distances between the trailing edges of the flaps were investigated (table II):

TABLE II

$2s_1$ (mm)	300	200	100	50	25
$\frac{s_1}{c}$	0.75	0.50	0.25	0.125	0.0625

The distance $2s_1 = 10$ millimeters could not be investigated since the strong jolting of the wings made it impossible to obtain sufficiently good measurements of the values of the aerodynamic forces.

In the tests the lift force, the drag, and the pitching moment were measured with respect to the nose of the profile at various angles of attack and various heights above the ground for the flapped and unflapped wings.

Together with the measurement of the forces and moments for the tests with and without flaps, the pressure distribution at one section of the upper wing was obtained over the surface of the profile. The section was taken at the distance 100 millimeters $(0.2\frac{b}{2})$ from the middle section of the wing in order to avoid the effect of the supports. For the wing without flaps at the surface of the profile 24 points were chosen at which the pressures were measured. For the case of the wing with open flaps 4 additional points were taken at the lower surface of the flap (fig. 14). Also, all the characteristics of the isolated wing corresponding to the case $2s = \infty$ and $2s_1 = \infty$ were obtained.

In analyzing the test results, the mean downwash of the wind-tunnel flow was taken into account. This correction was introduced also in the setting angle of the model of the upper wing. For the isolated wing the induction of the wind tunnel was taken into account in the usual manner. For the mirror reflection the computations showed that the correction on the induction of the wind tunnel was very small and could be neglected (reference 4). The tests were conducted in February 1938.

LIFT, DRAG, AND MOMENT OF LONGITUDINAL STABILITY

Wing without Flap

Figure 1 gives the curves of the lift coefficient against angle of attack. Each of the curves corresponds to a fixed distance between the trailing edges of the wings. Judging by the obtained test results, the change in the lift force in horizontal steady motion very near the ground as compared with flight far above the ground reduces essentially to the following:

(a) There is a change in the angle of attack corresponding to zero lift. For $\frac{s}{c} > 0.5$ this change is very small and may be essentially neglected. This shows that for these distances above the ground the effect of the profile thickness is small. Furthermore, with decrease in the distance $2s$ the displacement of the angle of zero lift begins to increase rapidly and for $\frac{s}{c} = 0.125$ for the given profile with $\bar{h} = 0.12$ it attains a value approximately equal to 2° (fig. 1).

(b) For small angles of attack near that corresponding to zero lift there is a certain decrease in the lift as compared with its values for the isolated wing. However, further on and up to angles immediately preceding the start of separation, there is a very considerable increase in the lift.[1]

(c) At small values of C_L with decrease in s there is a considerable increase in the derivative $\partial C_L / \partial \alpha$ and, for example, for $C_L = 0$ for $\frac{s}{c} = 0.25$, $\frac{\partial C_L}{\partial \alpha} = 7.96$, while for the isolated wing $\frac{\partial C_L}{\partial \alpha} = 3.73$.

(d) For $\alpha = 4 - 12^\circ$ the increase in the lift force coefficient ΔC_L depends little on the angle of attack. Below is given the mean values of the increments in the above-mentioned range of angles of attack:

$\frac{s}{c}$	0.75	0.50	0.25	0.125	0.0625	0.025
ΔC_L	0.105	0.145	0.220	0.295	0.380	0.475

[1] The comparison with the approximate theoretical computation is given in appendix I.

(e) The change in the maximum lift coefficient differs very greatly from the changes in the lift coefficient at "medium" angles of attack. Figure 2 shows the variation of ΔC_{Lmax} with $\frac{s}{c}$, where ΔC_{Lmax} is the increment of the maximum lift coefficient. For $\frac{s}{c} > 0.175$ there is a small decrease in C_{Lmax}. This drop at comparatively large distances has been confirmed by a large number of other tests. (See references 5 and 3.) During the flow of air between the wing and the ground there is an increase of pressure at the lower surface of the profile, and for very small distances this increase in pressure is very large. At medium angles of attack it leads directly to a general increase in the lift. Simultaneously, however, with an increase in the pressure at the lower surface there is a decrease in the pressure at the upper surface near the leading edge and an increase in the unfavorable pressure gradient which leads to an earlier flow separation near the ground. At relatively large distances ($\frac{s}{c} \gtrsim 0.175$) the increase in pressure on the lower surface cannot entirely compensate for the sharp increase in pressure at the upper surface due to the early separation and for this reason a small drop in C_{Lmax} is obtained. If the distances are small, however, ($\frac{s}{c} < 0.175$) the increase in pressure at the lower surface is so large that it covers the increase in pressure at the upper surface notwithstanding the fact that the separation, as before, starts considerably earlier than in the case of the isolated wing. Thus, for the case of very small distances to the ground C_L may somewhat exceed C_{Lmax} of the isolated wing although at the upper surface the flow will already be entirely separated.

The above-mentioned facts are illustrated with sufficient clearness by the pressure distribution picture which is given below. In general, however, it may be said that judging by the tests in the wind tunnel for all practical values of the distance from the wing to the ground, the maximum lift coefficient for steady horizontal flight near the ground varies little, although at medium angles of attack a considerable increase in the lift force is observed.

The curves of C_L against $\frac{c}{s}$ for various angles have a very characteristic appearance. (See fig. 3.) For $\alpha = 2\text{–}12^\circ$ and $\frac{c}{s} \longrightarrow \infty$; that is, for $s \longrightarrow 0$ the value of C_L approaches asymptotically a certain finite value. (See reference 1.) For negative α with decrease in the distance the value of C_L drops sharply. At these angles, owing to the

"Venturi" effect, very large forces are produced pushing both models toward each other, so that for very small distances the test could not be conducted since the models "hit" against each other.

Figure 4 gives the curves of C_D against α. For medium angles of attack there is a great lowering of C_D as compared with its values for the isolated wing. On approaching the critical angles, the difference in the drags decreases and at angles near the critical, the curve C_D for a given s intersects the C_D curve of the isolated wing. This is explained by the earlier separation of flow near the ground. There is further observed a considerable increase in the drag. The angle of attack corresponding to the minimum drag increases. The polars given in figure 5 show that near the ground a very great increase in the wing efficiency is obtained.

To estimate the order of the error obtained in determining C_D and C_L due to incorrect mounting of the upper wing, special tests were conducted in which for a fixed value of the angle of attack of the lower wing, the angle of attack of the upper wing was measured within the range $\alpha_{uw} = \alpha_{lw} \pm 2^\circ$. The greatest effect of the incorrect mounting of the upper wing was found at angles near the critical for small distances.

The results for $\alpha = 14^\circ$ for $2s = 100$ millimeters are shown in figure 6. The error in the angle of attack setting of the upper wing was less than $\pm 0.5^\circ$[1]. On figure 6 (dotted curves) are shown the small errors in the values C_D and C_L. For more stable conditions of flow these errors are considerably less.

Figure 7 shows the curves of the pitching moment with respect to the nose of the profile for fixed values $2s$ against the angles of attack. The change of these curves for small and medium angles of attack with decreasing distance from the ground to a large extent resembles the variation C_L with α. There is a displacement to the right of the angle of attack corresponding to $C_M = 0$ and a considerable increase in C_M at medium angles of attack. Moreover, in connection with an increase in pressure at the rear half of the profile the increase in the moment with respect to the profile nose occurs also at large angles of attack, that is,

[1]This angle was controlled with the aid of an optical goniometer. The range $\pm 0.5^\circ$ is to be taken with reserve.

even at those angles for which the flow of the upper surface is already separated. At these angles there is a rearward displacement of the center of pressure. The curves of C_L against C_m (fig. 8) give a very small change as compared with the case $2s = \infty$.

Wing with Flaps

For all curves for $\delta_f = 60^\circ$ one general property is noted: namely, in passing from $2s_1 = \infty$ to $2s_1 = 300$ millimeters a very considerable change in the aerodynamic characteristics occurs. A subsequent decrease in the distance gives relatively smaller change in the characteristics.

In the case of the wing with flaps tha change in the lift curves (fig. 9) reduces to the following:

1. For angles of attack below stalling there is a parallel displacement of the curve of C_L against α to greater values of the lift coefficient.

2. The value of the maximum lift coefficient for horizontal steady flight near the ground of the wing with flaps is considerably lowered for all investigated distances above the ground. The maximum of the lift coefficient curve is displaced toward smaller angles of attack.

The maximum decrease in C_{Lmax} occurs in passing from $2s_1 = \infty$ to $2s_1 = 300$ millimeters, but the further changes in C_{Lmax} are small. This result agrees well with the measured pressure distribution. At large angles of attack for $2s_1 = 300$ millimeters the pressure coefficient $\bar{p}$ at the lower surface differs little from $\bar{p} = 1$; that is, the flow is almost entirely stopped. There remain only very small possibilities for further increase in the pressure at the lower surface. For this reason, however small the distance between the trailing edges of the flaps, this small reserve of a possible increase in the pressures on the lower surface cannot, of course, compensate for the drop in lift resulting from the earlier flow separation on the upper surface due to the increase in the unfavorable pressure gradient.

Figure 10 shows the change in the drag coefficient of the wing with the flap. There is a considerable decrease in the drag at the angles of attack below stalling. After the

occurrence of separation there is a sharp increase in the drag of the wing. At small angles of attack the magnitude $\frac{\partial c_n}{\partial \alpha}$ considerably decreases. On figure 11 are constructed the polars for the wing with flap showing as in the case with the wing without the flap a very considerable increase in the efficiency.

The curves of the moment coefficient against the angle of attack (fig. 12) give for very small distances a rather large scatter. This is explained by the vibrating of the model and the inaccuracy resulting from this in measuring the force applied to the tail support. In contrast with the curves of C_m against α for the wing without flaps in the given case; that is, for the wing with flaps there is a decrease in the maximum value of C_m. This fact, like the drop in C_{Lmax}, is associated with the fact that the pressures at the lower surface are near the dynamic pressures and their range of further change is restricted. Thus the drop of the maximum value of C_m is explained by the considerable drop in the force C_L at a relatively small rearward displacement of the center of pressure. The curves of C_L against C_m (fig. 13) show only small changes as compared with the case of flight far above the ground.

PRESSURE DISTRIBUTION

The pressure distribution was determined parallel with the main tests on the force measurement. The pressures were measured on the upper wing at one section at a distance of 100 millimeters ($0.2 \frac{b}{2}$) from the middle section of the wing. Figure 14 shows the scheme of orifice location at this section. The distances x for the points at which the pressures were measured are given in table 3:

TABLE 3

Points	1	2	3	4	5	6	7	8	9	10	11	12	13	14
x (mm)	1	4	8	17	30	60	80	100	120	140	160	185	176	165.5
Points	15	16	17	18	19	20	21	22	23	24	25	26	27	28
x (mm)	157	148	128	107	100	60	30	17	9	4	1.74	132.5	192	198

The pressures were measured at 24 points on the surface of the profile and at 4 points on the outer part of the flap. Thus in the tests with the flap point No. 13 was located between the wing and the flap. The reading of the pressures at all points was conducted with the aid of a multiple monometer. The measurements were evaluated by the formula

$$\bar{p} = \frac{p_{loc} - p_{st}}{\rho \frac{v^2}{2}}$$

where p_{loc} is the local pressure at the surface of the profile and p_{st} is the static pressure outside the flow assumed equal to the static pressure in the flow.

On all pressure distribution curves the values of the nondimensional pressure coefficient $\bar{p}$ on the upper and lower surfaces of the wing were laid off. In figures 15 to 18 are given the pressure distributions for four angles of attack (case of the wing without flaps). For $\alpha = -4^\circ$ (fig. 15) a large force was produced which impelled both wings toward each other. The coefficient $\bar{p}$ on the lower surface attained large negative values.

Examination of figures 16 and 17 ($\alpha = 6^\circ$ and 10°) permits drawing an important conclusion. It is generally assumed that the effect of nearness to the ground is equivalent to a change in the true angle of attack. This conclusion is arrived at on analyzing, by the method of images, the curves of C_L and C_D against α for relatively large distances ($\frac{s}{c} > \frac{1}{2}$). The obtained picture of the pressure distribution shows, however, that the changes occurring near the ground are in no way equivalent to a change in the angle of attack. From figures 16 and 17 it is seen that over the linear portion of the change in C_L on decreasing the distance between the models, an entirely different pressure change is observed on the upper and lower surfaces than on increasing the angle of attack. On the upper surface for these angles of attack the pressure changes are insignificant and consist mainly of a decrease in $\bar{p}$ near the leading edge and an increase in $\bar{p}$ near the trailing edge. Over the entire lower surface there is a very considerable increase in pressure. Thus, it is seen that the ground effect must not be considered as equivalent to a change in the true angle of attack. Agreement in the value of the lift with the formulas taking account only of the effect of the vortex sheet of the upper wing (references

6 and 3) may be expected only for the case of large distances ($\frac{s}{c} > 1$), where in general the changes in the aerodynamic characteristics are not large. Thus, even for the approximate computation of the change in C_L the finiteness of the chord and the thickness of the profile must be taken into account. The computations given in the appendix show that this may be done with sufficient accuracy only for $\frac{s}{c} > \frac{1}{3}$. As regards the change in the drag for $\frac{s}{c} > \frac{1}{3}$, it is necessary to take into account only the induced drag. For below-stalling angles of attack good qualitative agreement is obtained.

Figure 18 ($\alpha = 14^\circ$) confirms what has been remarked above with regard to the change in $C_{L\max}$ in horizontal steady flight near the ground. It is seen on this figure that premature flow separation is obtained on the upper surface while on the lower surface there is a very sharp increase in pressure. For $\frac{s}{c} > 0.175$ this increase in the pressure cannot compensate for the loss of lift due to the separation from the upper surface. For $\frac{s}{c} < 0.175$ the increase in the pressures on the lower surface is so great that a small increase in C_L is obtained as compared with the value of $C_{L\max}$ for $2s = -\infty$ although the flow of the upper surface is already completely separated. By planimetering the curves of pressure distribution for all the angles of attack and distances investigated, the curves of local normal lift coefficients (C_z) against the angles of attack for fixed values of 2s could be drawn (fig. 19). These curves give qualitatively the same picture as the curves of C_L against α (fig. 1). The curves of the local normal force coefficient may be drawn separately for the upper surface (fig. 20) and the lower surface (fig. 21). Figure 21 shows what a considerable increase in the lift force is obtained as a result of the increase in pressure at the lower surface of the profile. The breaks in these curves (fig. 20) correspond to the start of flow separation at the upper surface; while for small distances, when the gap between the wings was small, separation at the upper surface gave essentially only a small effect on the lower surface. It is here also seen that with further decrease in the gap the value of the local normal lift coefficient at the lower surface ($C_{z_{ls}}$) approaches unity. Figure 21 shows that at angles of attack below stalling for all distances, the changes in the local normal force coefficient at the upper surface are small. The separation at the upper surface starts earlier than for the case of flight far above the ground.

Figures 22 and 23 show the pressure distribution for the wing with flaps for $\alpha = -4^{\circ}$ (fig. 22) and $\alpha = 6^{\circ}$ (fig. 23). In the region between the wing and the flap the pressure was measured at only one point, and for this reason it was not possible on the curves to give the pressure distribution of the parts corresponding to this region. This region has only a small effect on the total value of the local normal force coefficient and account is taken of it approximately by making use of the detailed investigation of the pressure distribution for such profile. (See reference 7.) The greatest changes in pressure occur in passing from the isolated wing to the distance $2s_1 = 300$ millimeters. At the upper surface near the leading edge the pressure decreases.

On figure 23 it is seen that for $\alpha = 6^{\circ}$ for the distances $2s_1 = 50$ and $2s_1 = 25$ millimeters separation has already started. For this angle of attack it is very clearly seen that the possibilities of further increasing the pressures at the lower surface are not large. For example, for $2s_1 = 25$ millimeters the pressure almost everywhere attains practically its limiting value ($\bar{p} = 1$).

The curves of local normal force coefficient against angle of attack given in figure 24 were obtained by planimetering the curves of pressure distribution. They confirm the qualitative results obtained on the basis of the curves of C_L against α. In figures 25 and 26 these curves were drawn separately for the upper and lower surfaces. The small increase in C_{zus} for angles of attack below stalling (fig. 25) as compared with flight far above the ground is connected with the fact that the decrease in $\bar{p}$ near the leading edge in the case of flaps is not entirely compensated by the increase in $\bar{p}$ near the trailing edge. It is of interest to note that at very small distances the values of the local normal force coefficient for the lower surface C_{zls} depends little on the angle of attack (fig. 26).

CONCLUSIONS

1. In the case of horizontal steady flight at small heights above the ground at below stalling angles of attack the lift force very considerably increases and the drag decreases. An exception occurs in the case of negative and small positive angles for which owing to an effect analogous to the "venturi tube" effect, a considerable force is produced that draws the wing to the ground.

2. In horizontal flight near the ground the flow separation at the upper surface occurs at smaller angles of attack than in flight far above the ground.

3. For all practical values of the distances above the ground in horizontal steady flight, the value of C_{Lmax} of the wing without flaps changes very little. This conclusion must not, of course, be extended to the process of landing of the airplane where, on account of the rotational motion of the wing and the effect of the unsteady flow on approaching the ground, an additional increase in the lift is obtained mainly near the value of C_{Lmax}.

4. For a wing with flaps there is likewise an increase in the lift for angles of attack below stalling and a decrease in the drag. The separation occurs at a considerably smaller angle of attack than in flight far above the ground.

5. For the wing with flap in horizontal steady flight near the ground, there is a considerable lowering in C_{Lmax}.

6. Investigation of the pressure distribution for the wing without flap showed that for angles of attack below stalling on decreasing the distance above the ground, the character of the pressure changes on the upper and lower surfaces is found to be quite other than on increasing the angle of attack. At the upper surface the changes are slight and reduce mainly to an increase in the unfavorable pressure gradient leading to earlier flow separation. At the lower surface with decrease in the distance there is a very sharp pressure increase, which determines the obtained increase in the lift.

7. For flight with fully opened flap it was found that on decreasing the distance from the trailing edge of the flap to the ground up to a value of the order of 0.5 chord for angles of attack near the critical, the values of the pressures at the lower surface on account of the very strong retardation of the flow, are near the limiting value, that is, the flow is almost entirely stopped.

8. The changes in the curves of C_m against C_L both for the wing without flap and for the wing with flap are small as compared with flight far above the ground.

APPENDIX

It may be assumed that the change in the aerodynamic characteristics of a monoplane wing in horizontal steady flight near the ground is determined by three factors: (1) the effect of the system of free vortices of the reflected wing, (2) the effect of the width of the chord, and (3) the effect of the thickness of the profile. Such consideration is, of course, a first approximation in the solution of the problem since the effect of the shape of the profile is not taken into account. The proposed scheme of computation is to a considerable degree justified by the fact that satisfactory agreement is obtained with the results of experiment for distances from the axis of the bound vortex to the ground $H > \frac{c}{2}$. The formulas are valid only for the linear part of the lift curve C_L against α. Let

$$\Delta C_L = \Delta C_{L_1} + \Delta C_{L_2} + \Delta C_{L_3} \tag{1}$$

where

ΔC_L the total correction which is added to the lift coefficient of the wing flying high above the ground

ΔC_{L_1} the correction for the effect of the system of free vortices of the reflected wing

ΔC_{L_2} the correction for the width of the chord

ΔC_{L_3} the correction for the thickness of the profile

1. Determination of ΔC_{L_1}:

$$\Delta C_{L_1} = \frac{a\sigma}{\pi\lambda} C_L$$

where

$$a = \frac{a_0}{1 + \frac{a_0(1+\sigma)}{\pi\lambda}}$$

that is

$$\Delta C_{L_1} = \frac{a_0\sigma}{\pi\lambda + a_0(1-\sigma)} C_L \tag{2}$$

The values of σ are given in figure 27. (See reference 6.)

2. Determination of ΔC_{L_2}:

To determine the effect of the width of the chord the theory of the thin airfoil was applied. The solution is considerably simplified if the first two terms of the series are limited to giving the distribution of the circulation over the chord.

The condition of equating to zero the normal velocity along the chord may be written in the form

$$v \sin \alpha + w_1 + w_2 = 0$$

where w_1 is the normal velocity produced by the vortex system of the wing at a certain point of the chord with the abscissa x and w_2 the normal velocity at the same point induced by the vortex system of the reflected wing.

On satisfying this relation for two points (e.g., $x = 0$ and $x = c$) a system of linear equations may be arrived at from which the two unknown coefficients for the circulation series A_0 and A_1 are determined. Without making all the intermediate computations, the formula for determining ΔC_{L_2} is given:

$$\Delta C_{L_2} = r(\gamma - 1)\, C_L \tag{3}$$

where

$$r = \sqrt{1 + \frac{4H}{b_2}} - \frac{2H}{b}, \quad \gamma = \frac{\gamma_1}{a_0}$$

The values of γ_1 are given in figure 28.

3. Determination of ΔC_{L_3} (reference 5):

$$\Delta C_{L_3} = - a_0 k \bar{h} \tag{4}$$

where

$$k = 0.003 \frac{H}{c} \left\{ \frac{1}{\left(\frac{H^2}{c^2} + \frac{1}{64} \right)^2} + \frac{3}{\left(\frac{H^2}{c^2} + \frac{9}{64} \right)^2} \right\}$$

The correction ΔC_{L_3} gives a parallel displacement of the C_L curve to the right.

Figures 29, 30, and 31, show a comparison of the values computed by these formulas with test results. The theoretical values of C_L, obtained by formula (1), are given by the continuous curves. In view of the fact that the theoretical curves are drawn for fixed values of H while the test was conducted for constant s, it was necessary to interpolate the test values (dot-dash). The comparison shows that for $\frac{H}{c} > 0.5$ the agreement obtained is satisfactory. For $\alpha > 0$ the values of H are greater than the corresponding values of s. It may be shown that for $\frac{s}{c} > \frac{1}{3}$ the computation by formula (1) gives satisfactory results.

On the same figures is given the computation according to Wieselsberger in which account was taken only of the correction ΔC_{L_1} (dotted curve). Bad agreement was obtained with experiment for the distances investigated. The formula of Wieselsberger may be used only for $\frac{s}{c} > 1$.

The correction on the drag for ground effect is very difficult to obtain in the case of small heights above the ground at negative and small positive angles (in this case $-4^\circ < \alpha < 2^\circ$) where there is also the venturi tube effect. The change in the drag due to ground effect for angles of attack below stalling may be approximately accounted for by the formula

$$\Delta C_D = \Delta\alpha \; C_L \qquad (5)$$

The computation by the above formula is conducted in the following manner:

1. Construct the curves of C_L against α for $H = \infty$ and for a certain fixed value of H by formula (1).

2. Draw the polar of the wing for $H = \infty$.

3. Redraw the polar. For this purpose, determine what equivalent increase in the angle of attack $\Delta\alpha$ is obtained in passing from the C_L curve for $H = \infty$ to the C_L curve constructed by formula (1) if C_L is constant. By multiplying the measured $\Delta\alpha$ by the corresponding C_L there is obtained by formula (5) the value of ΔC_D. The point of the polar taken for the same C_L to the left is displaced by an amount equal to ΔC_D.

Figures 29, 30, and 31 show the comparison of the polars obtained by formula (5) and the curves obtained by interpolating the test for the same H. There are also given the polars obtained by the Wieselsberger formula. The comparison shows that for $\frac{H}{c} > 0.5$ the agreement of the computation by formula (5) with experiment for below-stalling angles is sufficiently close.

For the case of the wing with flap the derivation of the general relations offers great difficulties. Here are given empirical formulas obtained on the basis of the analysis of the results of the test described above. They are true for $\delta_f = 60^\circ$ for angles of attack below stalling.

$$\left.\begin{aligned} \Delta C_L &= \frac{0.145 \frac{c}{s_1}}{0.27 \frac{c}{s_1} + 1} \\ \Delta C_D &= C_D \frac{0.155 \frac{c}{s_1}}{0.41 \frac{c}{s_1} + 1} \\ &\delta_f = 60^\circ \end{aligned}\right\} \qquad (7)$$

For the test here described these formulas give good agreement.

Translation by S. Reiss,
National Advisory Committee
for Aeronautics.

REFERENCES

1. Serebrisky, Y. M: The Effect on the Increase of the Lift Coefficient in the Rotational Motion of a Wing. Technika Vozdushnogo Flota No. 11, 1936.

2. Serebrisky, Y. M: Experimental Investigation of the Vertical Approach of a Plate and the Inclined Approach of a Wing to the Ground. CAHI Rep. No. 422, 1939.

3. Serebrisky, Y. M: The Effect of the Nearness to the Ground on the Aerodynamic Characteristics of an Airplane. CAHI Rep. No. 267, 1936.

4. Silverstein, Abe, and White, James A.: Wind-Tunnel Interference with Particular Reference to Off-Center Positions of the Wing and to the Downwash at the Tail. NACA Rep. No. 547, 1935.

5. Tani, Itiro, Taima, Masuo, and Simidu, Sodi: The Effect of Ground on the Aerodynamic Characteristics of a Monoplane Wing. Rep. of the A.R.I., Tokyo Imperial University, No. 156, (vol. 13, no. 2) 1937.

6. Wieselsberger, C: Wing Resistance near the Ground, NACA TM No. 77, 1922.

7. Wenzinger, Carl J.: Pressure Distribution over a Clark Y-H Airfoil Section with a Split Flap. NACA TN No. 627, 1937.

BIBLIOGRAPHY

Dätwyler, G.: Untersuchung über das Verhalten von tragflügelprofilen sehr nähe am Boden. Mitteilungen aus dem Institut für Aerodynamik, Eidgenössiche Technische Hochschule (Zürich) 1934.

Tomotika, Susumu, Nagamiya, Takeo, and Takenouti, Yositada: The Lift on a Flat Plate Placed near a Plane Wall, with Special Reference to the Effect of the Ground upon the Lift of Monoplane Aerofoil. Rep. of the A.R.I., Tokyo Imperial University, No. 97, (vol. 8, no. 1) 1933.

Ushakov, B. A.: Effect of Nearness to the Ground on the Aerodynamic Characteristics of the Wing. CAHI Tech. Note No. 47, 1935.

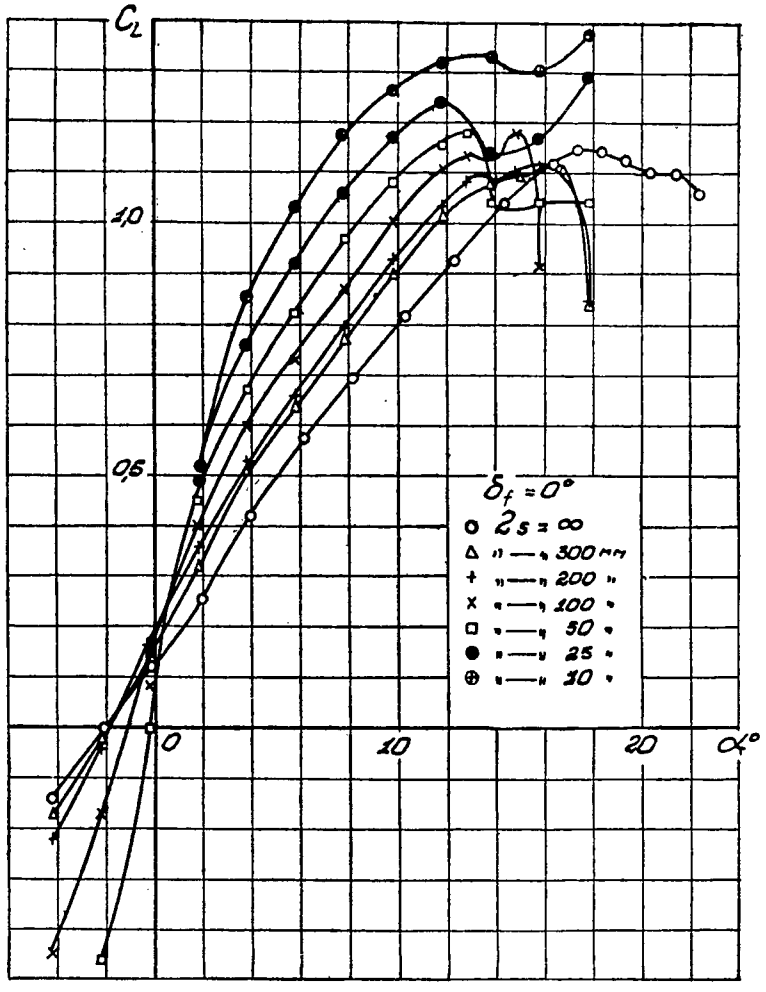

Fig.1

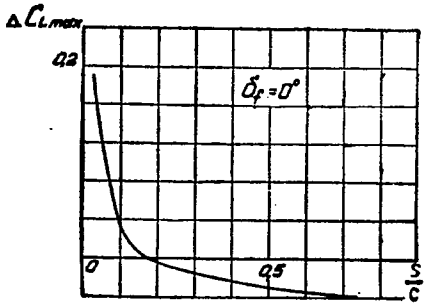

Fig.2

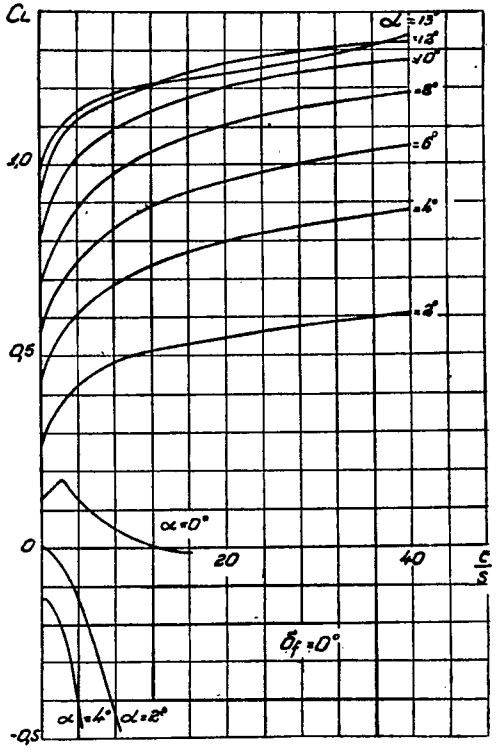

Fig. 3

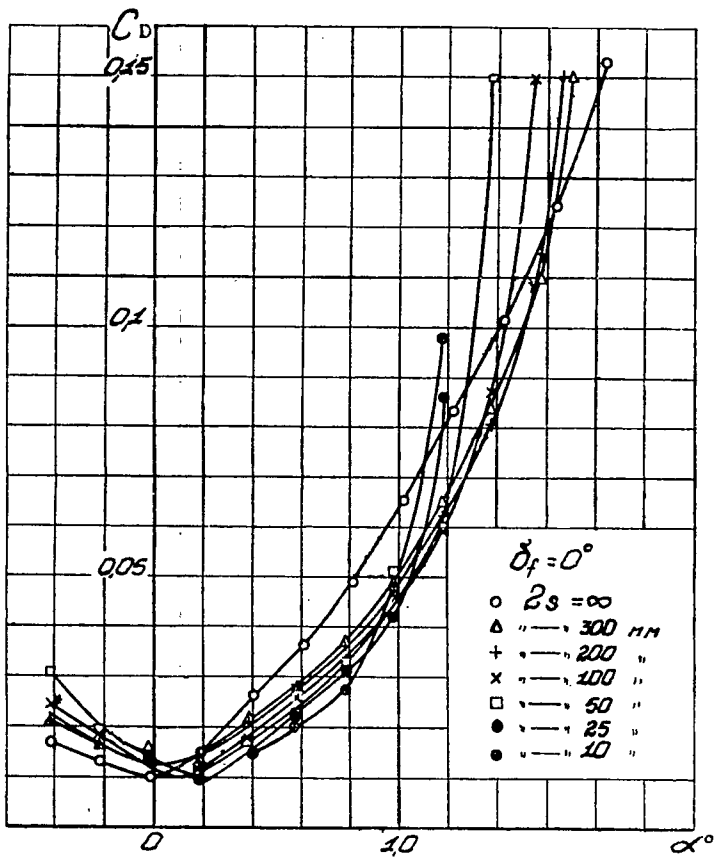
C_D
0,15
0,1
0,05
0
1,0
$\alpha°$
$\delta_f = 0°$
$2s = \infty$
300 mm
200 "
100 "
50 "
25 "
10 "

Fig. 4

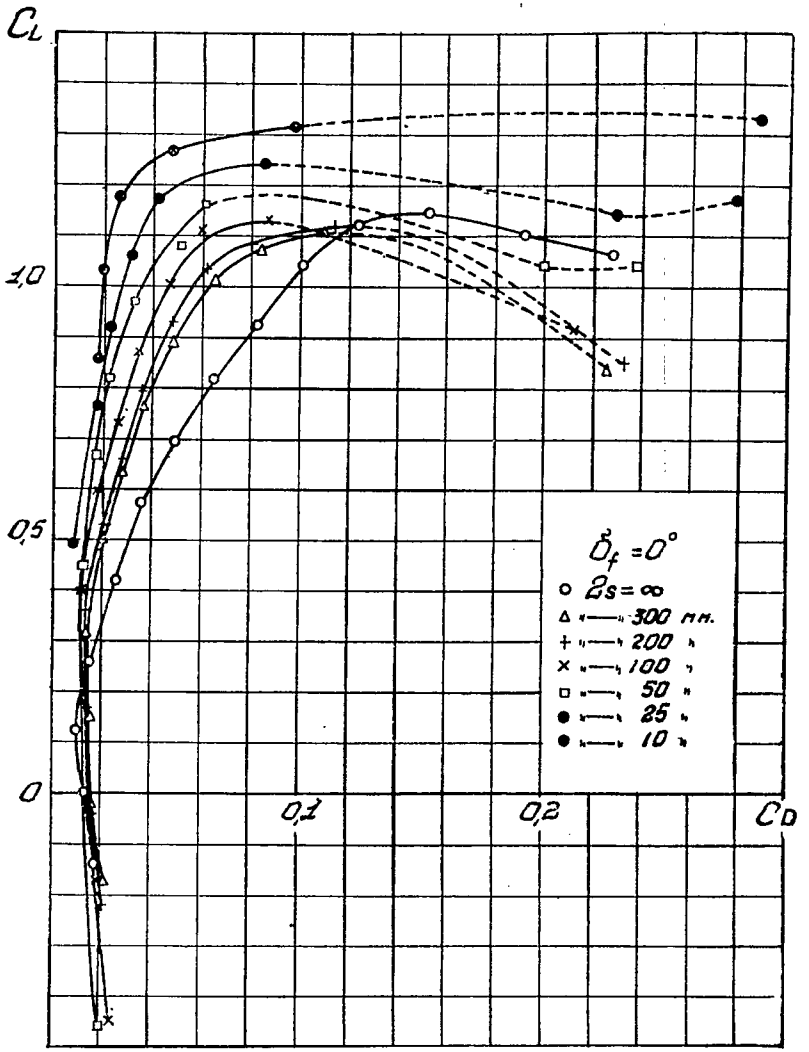
C_L
1,0
0,5
0
0,1
0,2
C_D
$\delta_f = 0°$
$2s = \infty$
300 mm.
200 "
100 "
50 "
25 "
10 "

Fig.5

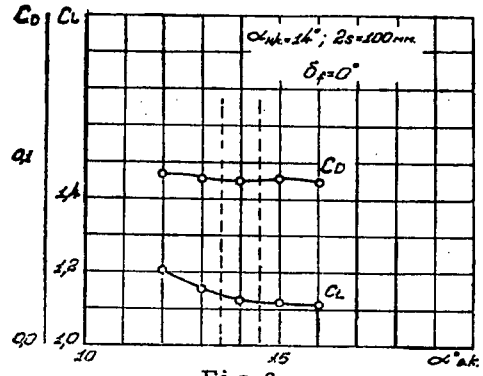

Fig. 6

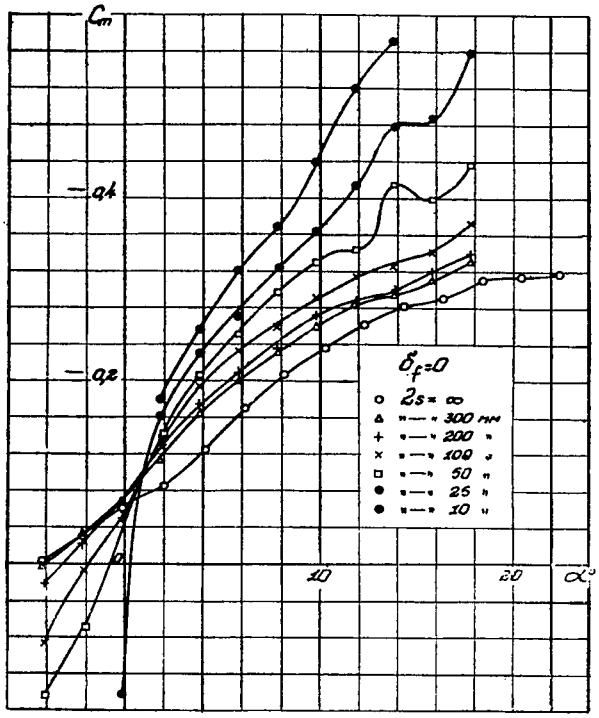

Fig. 7

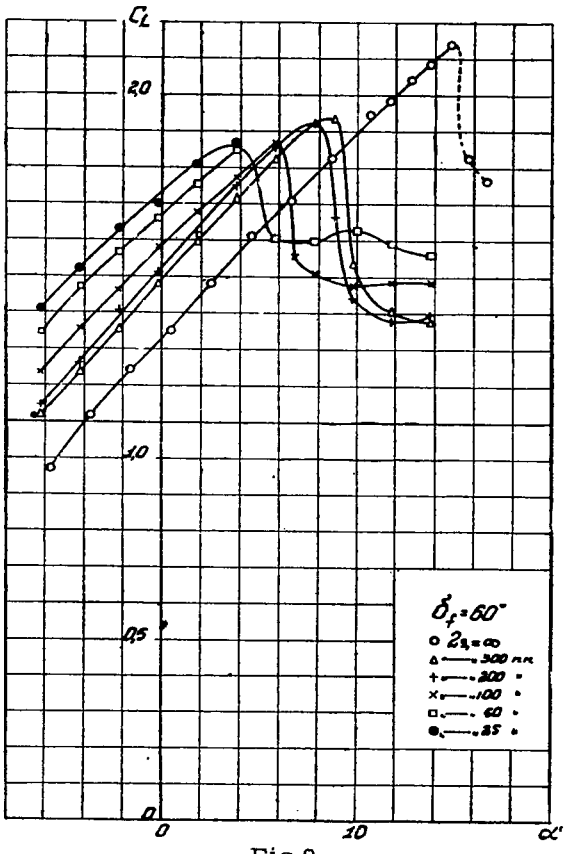

Fig. 9

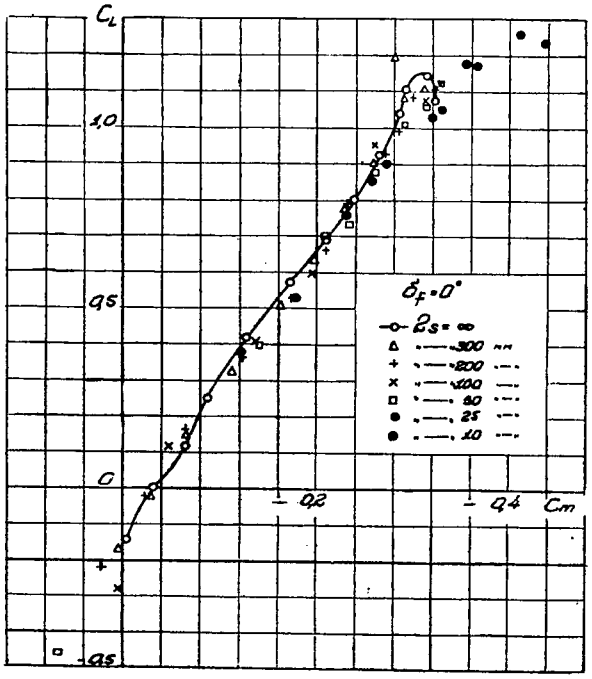

Fig. 8

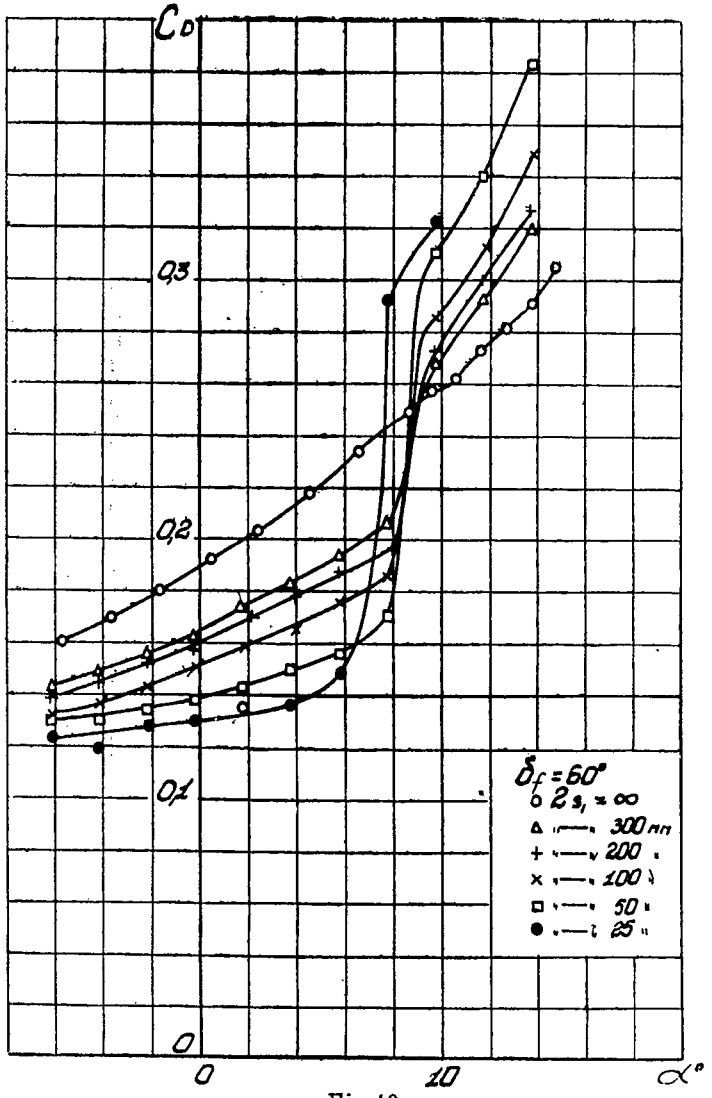
C_D
0,3
0,2
0,1
0
0
10
$\alpha°$
$\delta_f = 60°$
$2s_1 = \infty$
300 mm
200 "
100 "
50 "
25 "

Fig.10

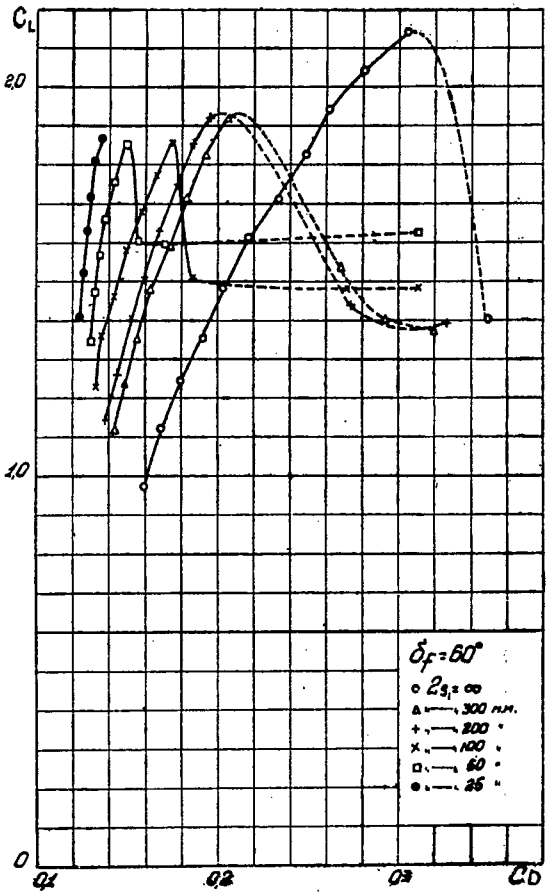
C_L
2,0
1,0
0
0,1
0,2
0,3
C_D
$\delta_f = 60°$
$2s_1 = \infty$
300 mm.
200 "
100 "
60 "
25 "

Fig. 11

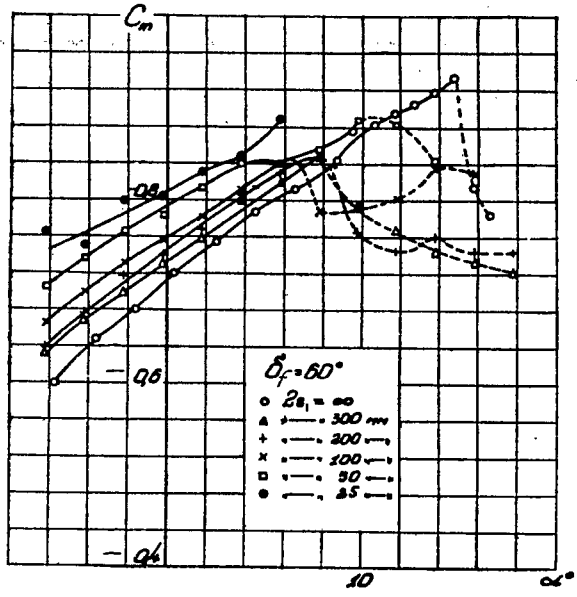

Fig. 12

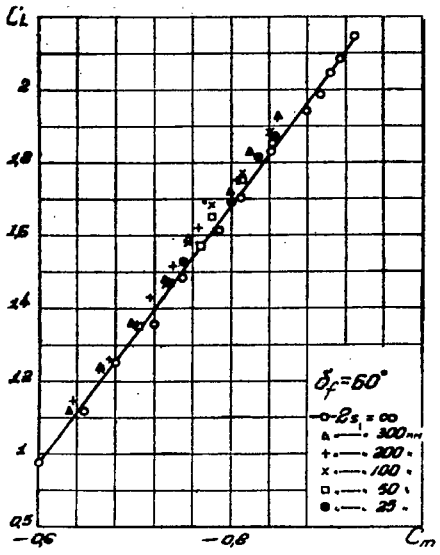

Fig. 13

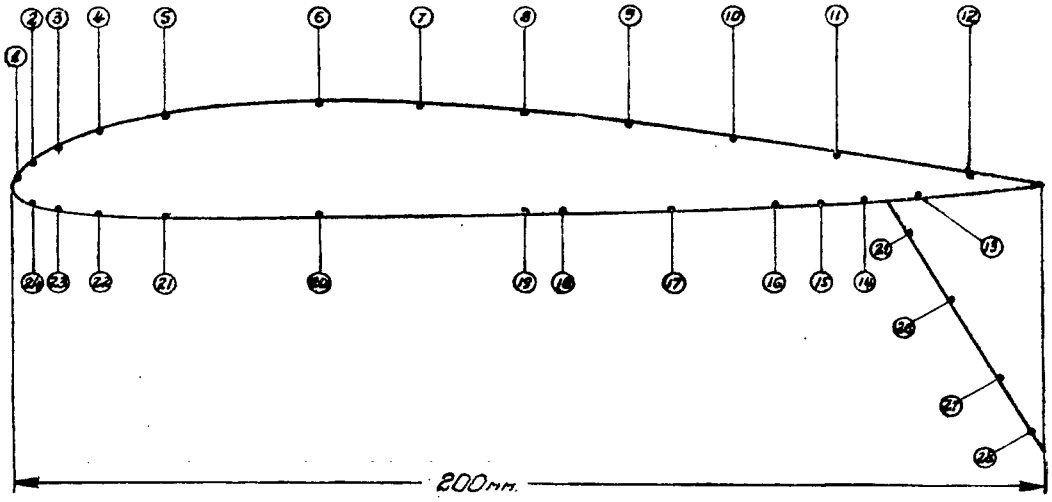

Fig. 14

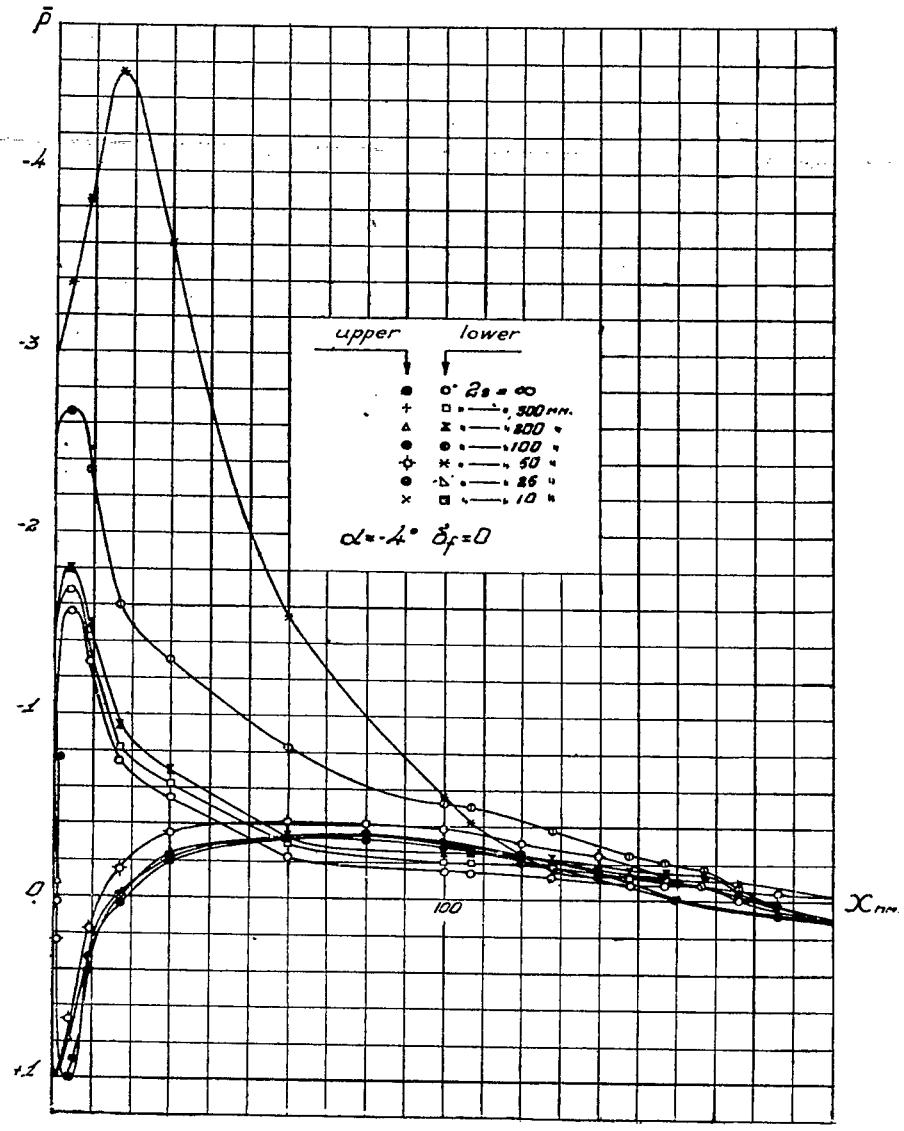
$\bar{p}$
-.4
-.3
-.2
-.1
0
.1
upper
lower
$\alpha = -4°$ $\delta_f = 0$
100
x_{mm}

Fig. 15

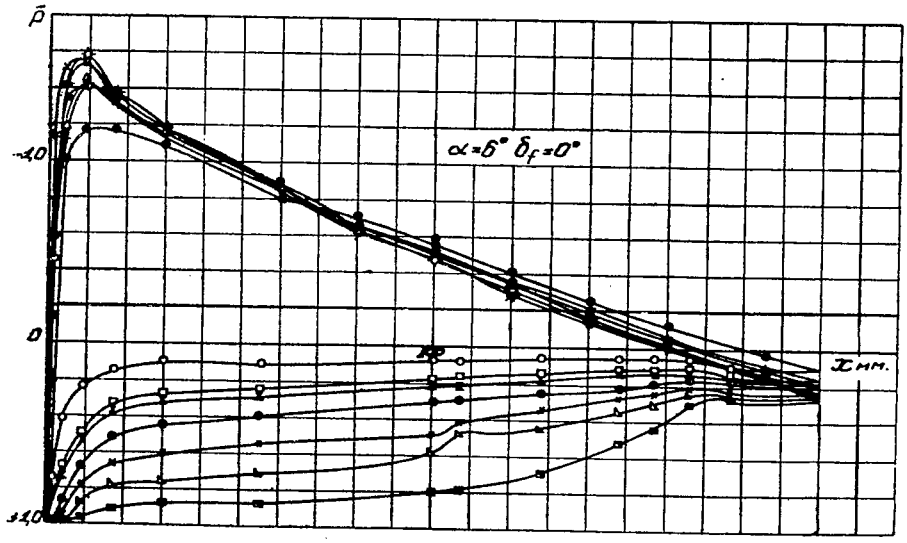
$\bar{p}$
-1.0
0
1.0
$\alpha = 6°$ $\delta_f = 0°$
100
x_{mm}

Fig. 16

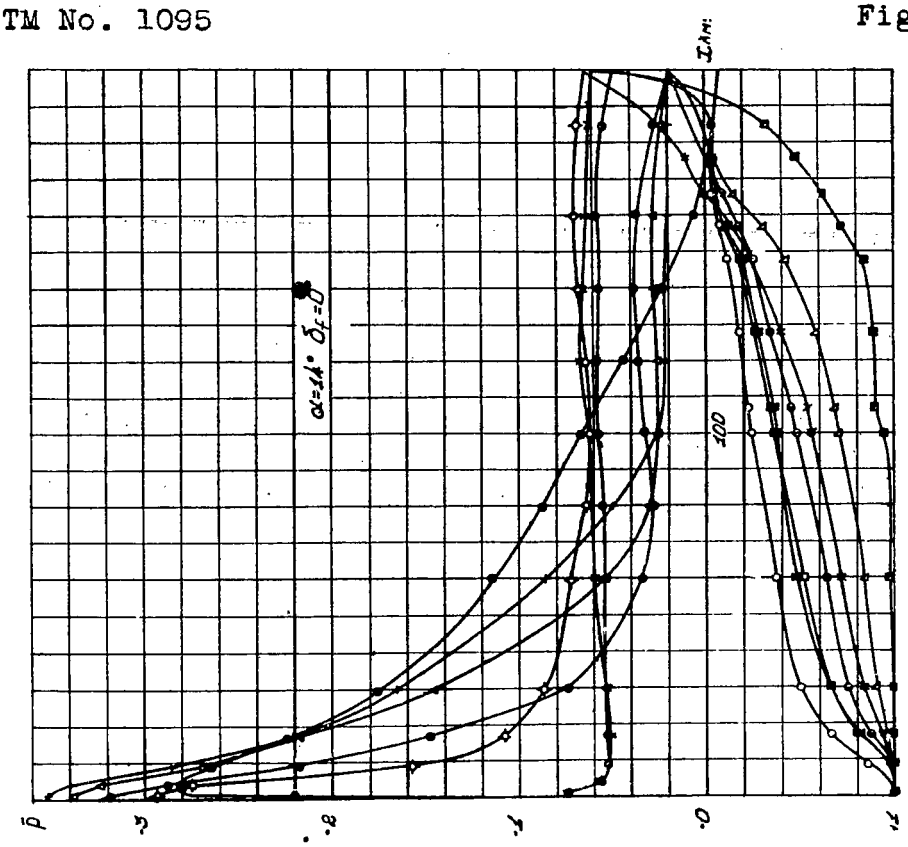
x_{mm}
$\alpha=14°$ $\delta_f=0°$
100
$\bar{p}$
-.4
-.8
-1.2
0
.4

Fig. 18

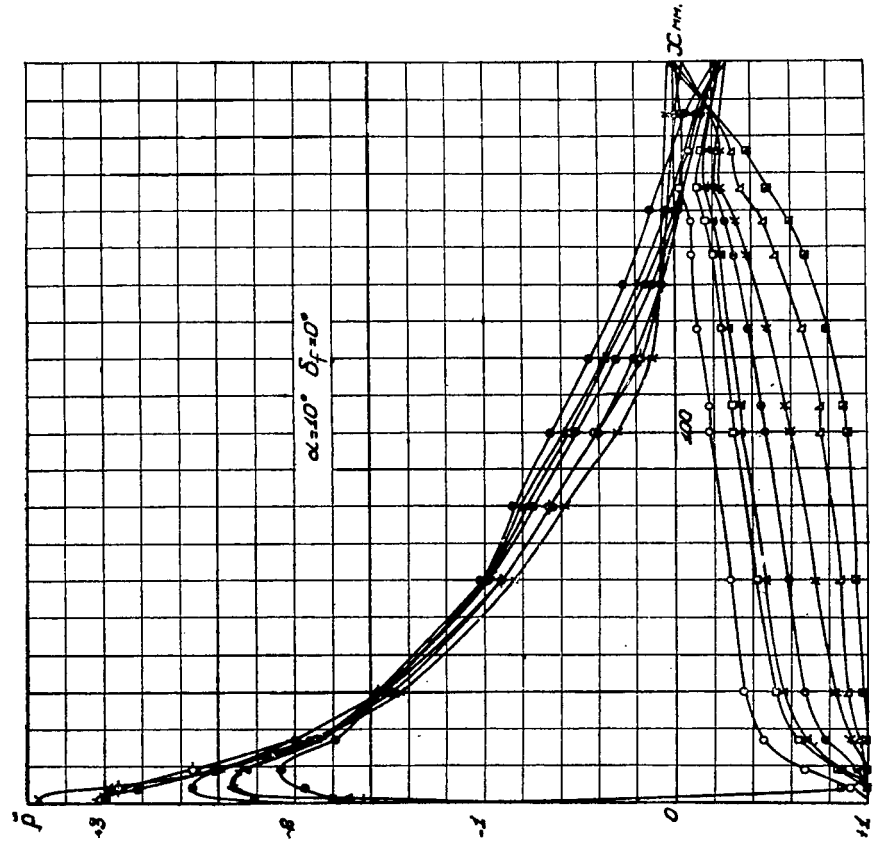
x_{mm}
$\alpha=10°$ $\delta_f=0°$
100
$\bar{p}$
-.4
-.8
-1.2
0
.4

Fig. 17

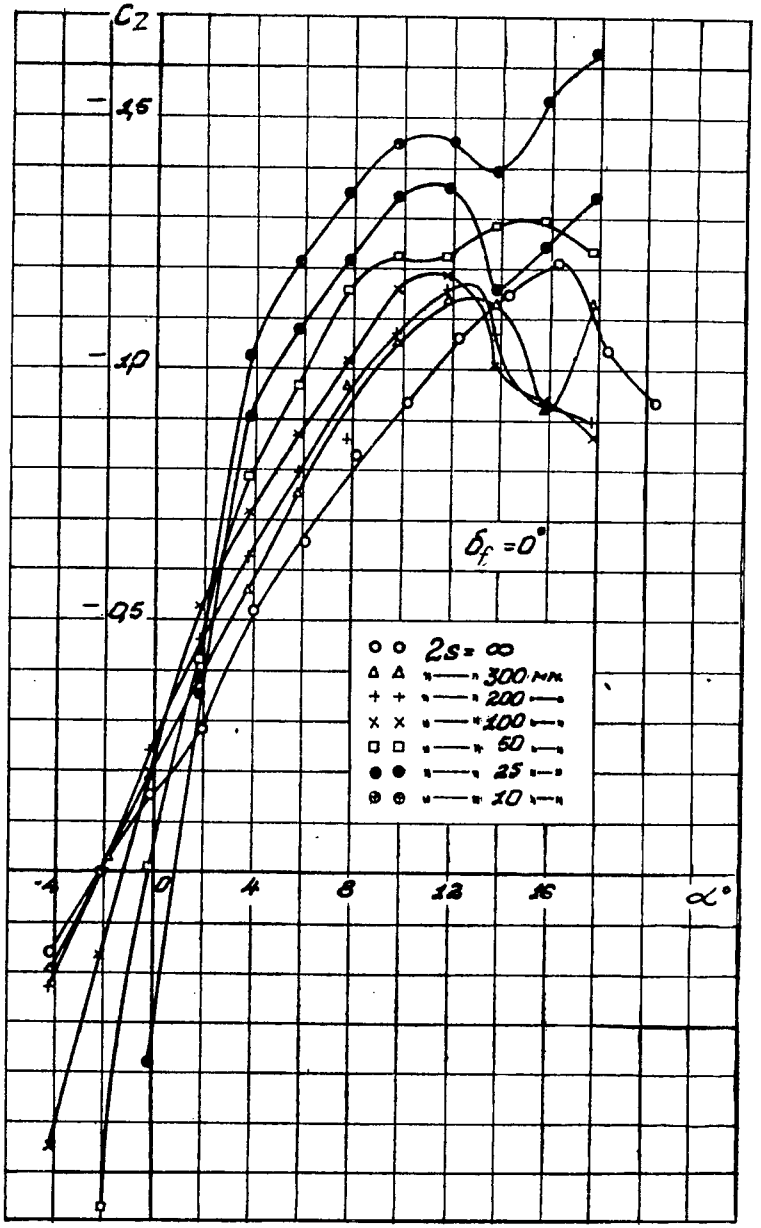
c_z
1,5
1,0
0,5
$\delta_f = 0°$
2s = ∞
300 мм
200
100
50
25
10
-4
0
4
8
12
16
α°

Fig. 19

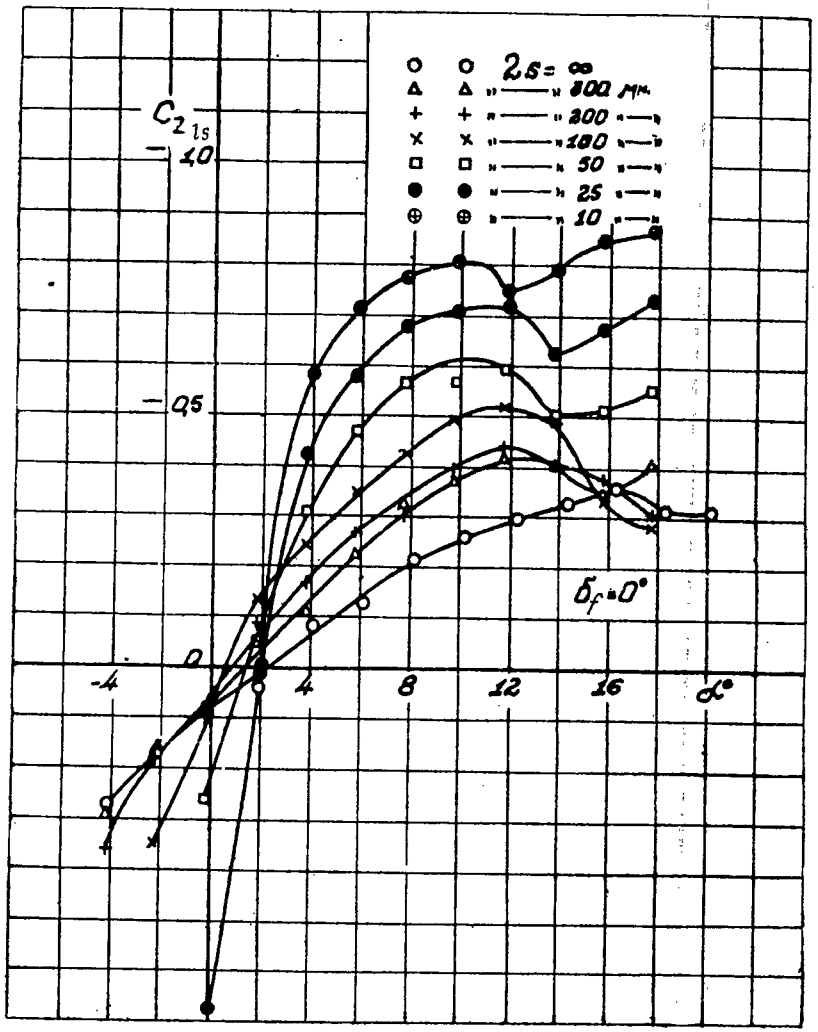
$c_{z\,1s}$
1,0
0,5
2s = ∞
300 мм
200
100
50
25
10
$\delta_f = 0°$
-4
0
4
8
12
16
α°

Fig. 20

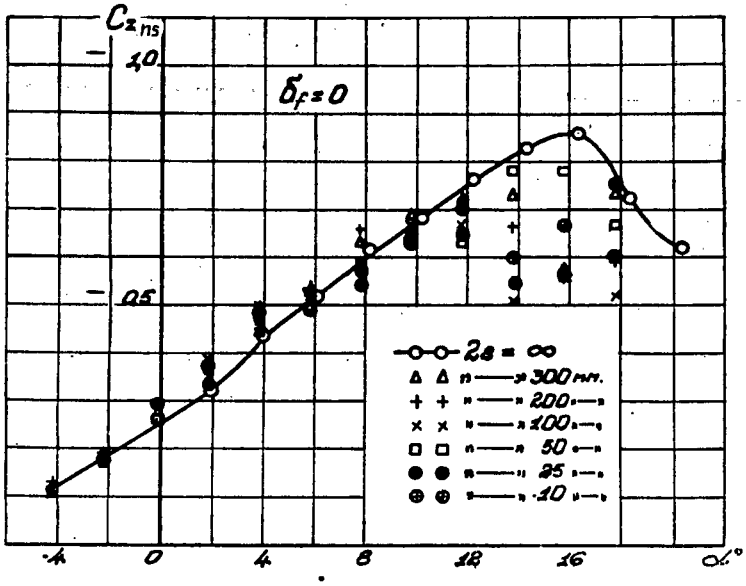
$C_{z\,ns}$
-1,0
-0,5
$\delta_f = 0$
$2s = \infty$
n = 300 mm.
n = 200 "
n = 100 "
n = 50 "
n = 25 "
n = 10 "
-4
0
4
8
12
16
α°

Fig. 21

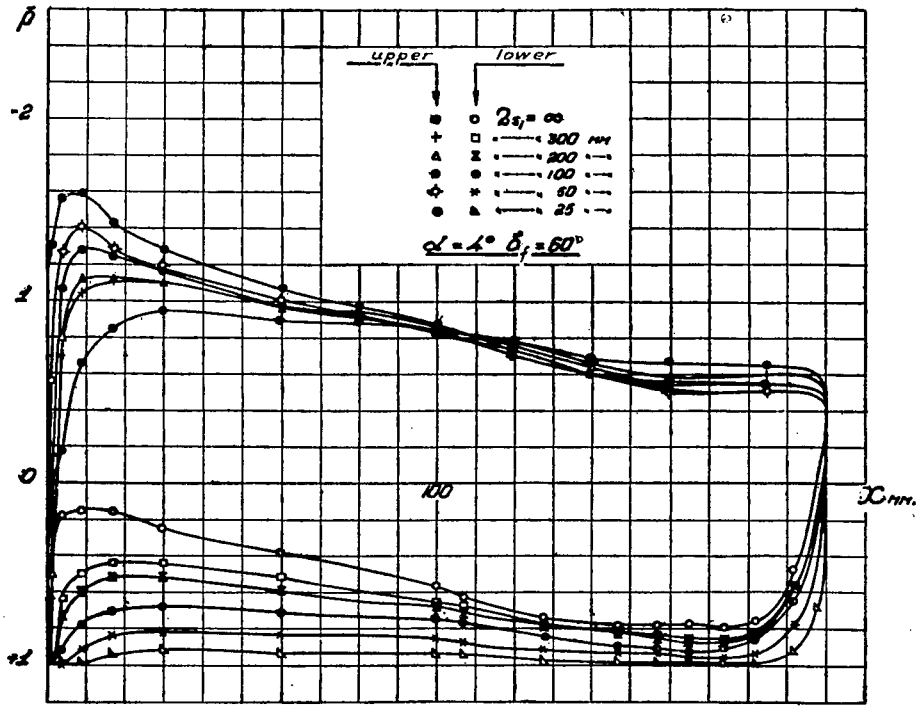
p̄
-2
1
0
+1
upper
lower
$2s_1 = \infty$
300 mm
200
100
50
25
$\alpha = 4°$ $\delta_f = 60°$
100
x mm.

Fig. 22

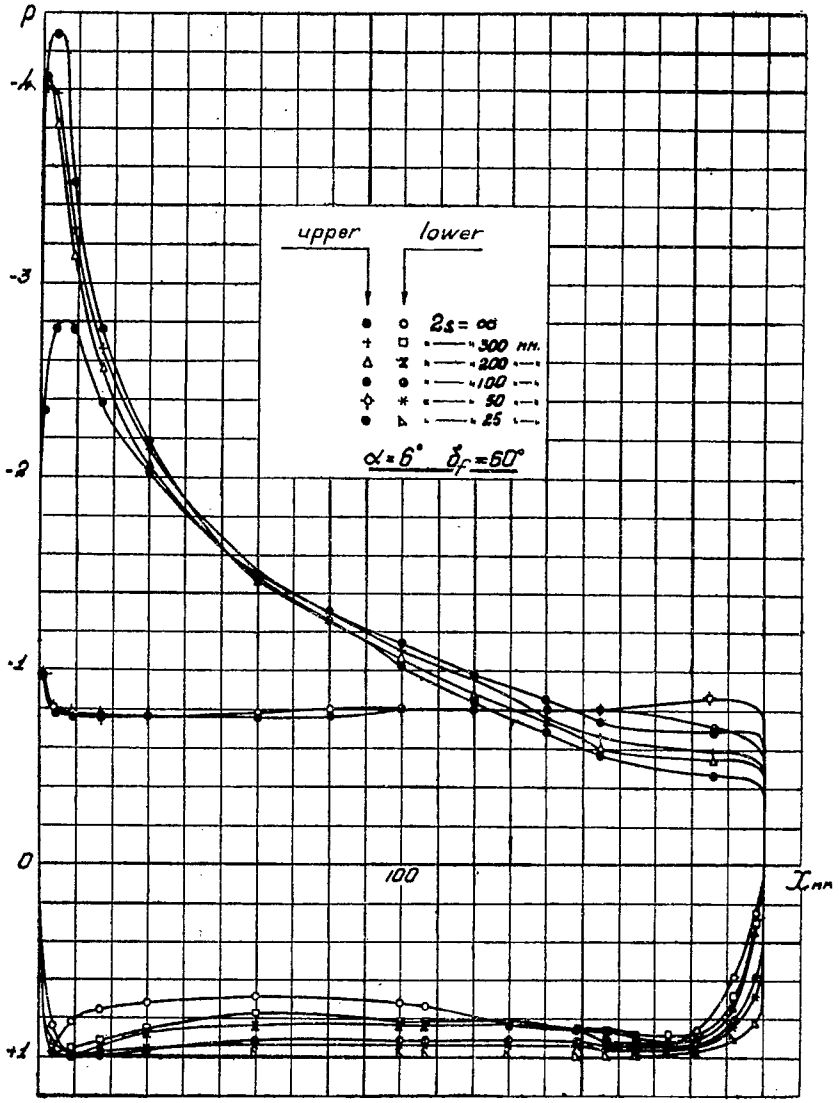
p
upper
lower
2s = ∞
" 300 mm.
" 200 "
" 100 "
" 50 "
" 25 "
α = 6° δf = 60°
100
x mm

Fig. 23

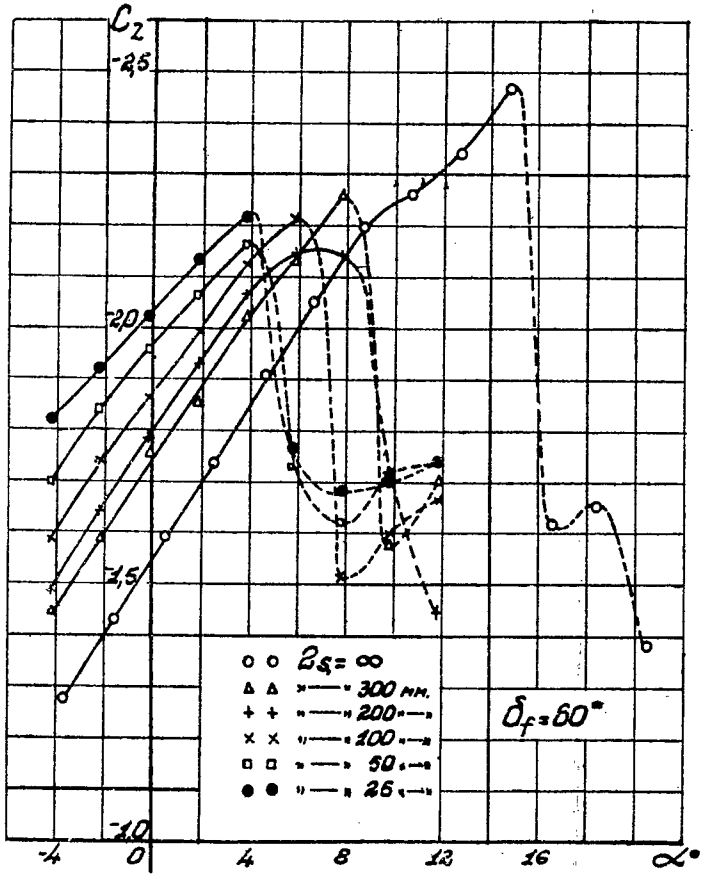
c2
2s = ∞
" 300 mm.
" 200 "
" 100 "
" 50 "
" 26 "
δf = 60°
α°

Fig. 24

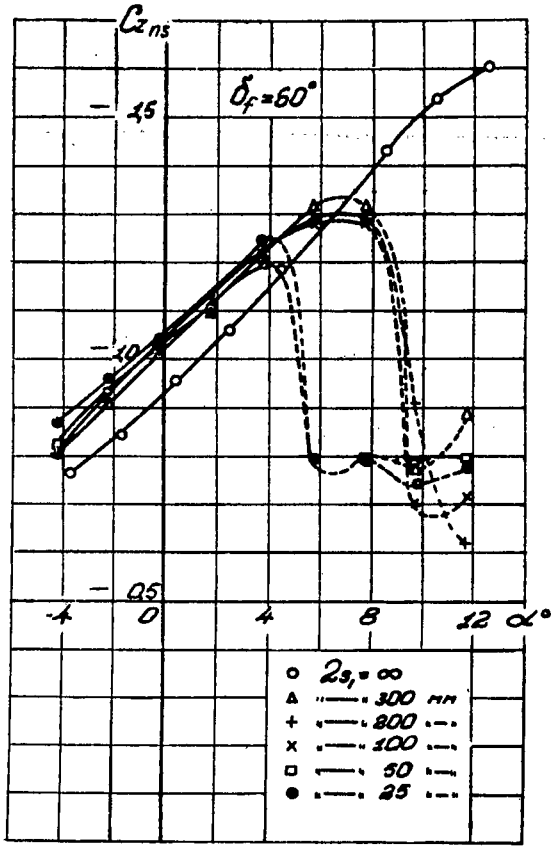

Fig. 25

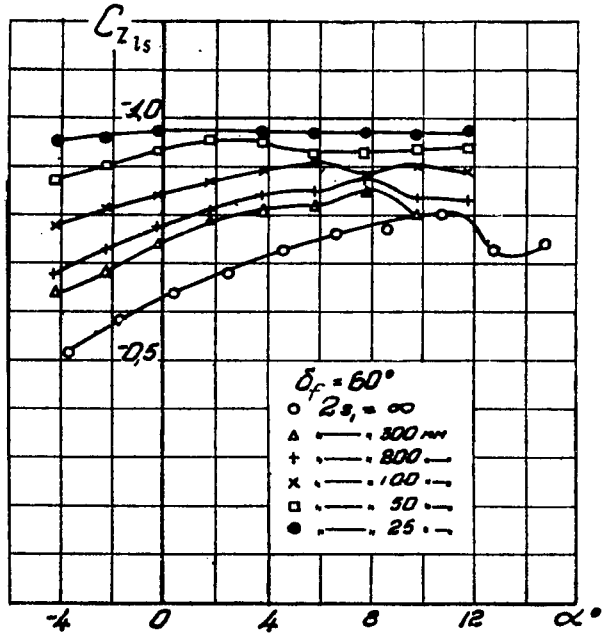

Fig. 26

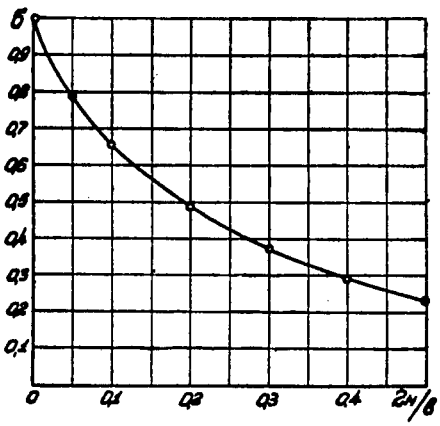

Fig. 27

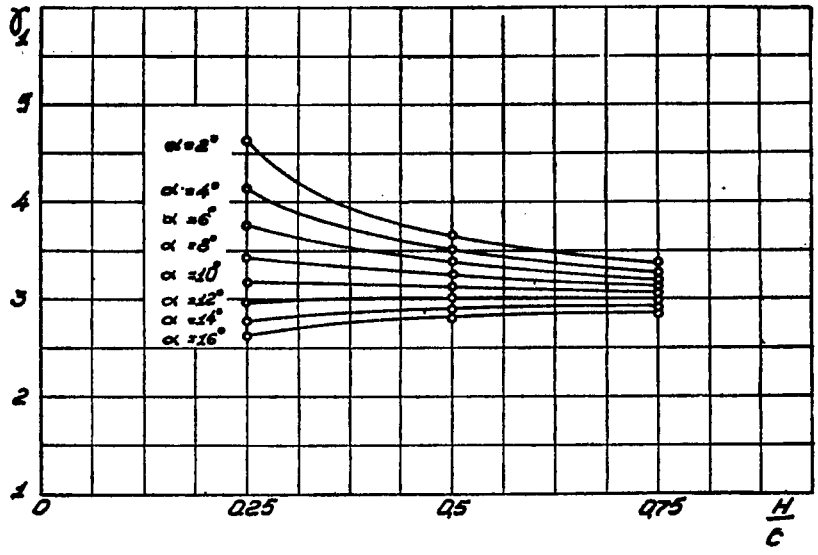
σ_1
5
4
3
2
1
0
0.25
0.5
0.75
$\frac{H}{c}$
α=2°
α=4°
α=6°
α=8°
α=10°
α=12°
α=14°
α=16°

Fig. 28

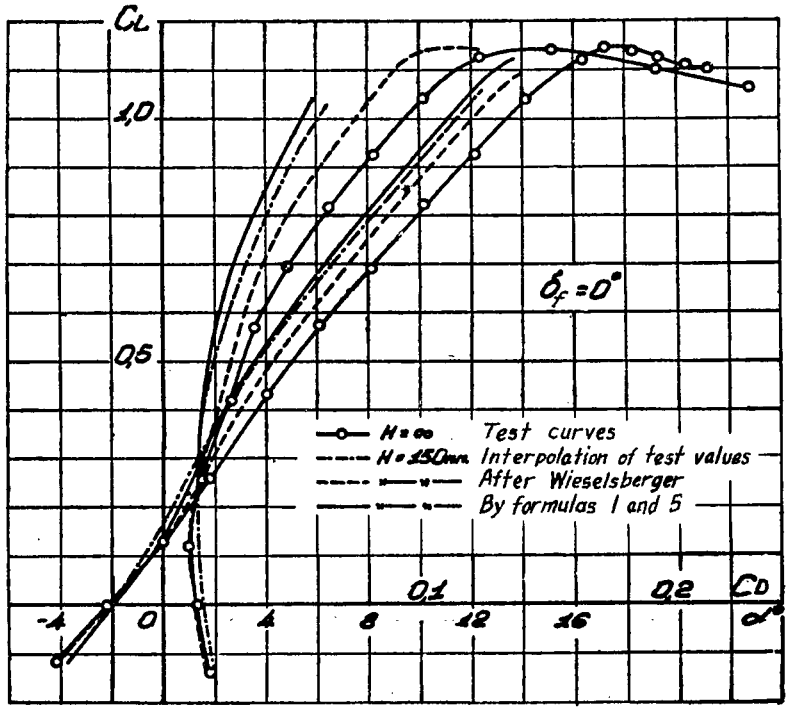
C_L
1.0
0.5
$\delta_f = 0°$
H = ∞ Test curves
H = 150mm Interpolation of test values
After Wieselsberger
By formulas 1 and 5
0.1
0.2
C_D
-4
0
4
8
12
16
α°

Fig. 29

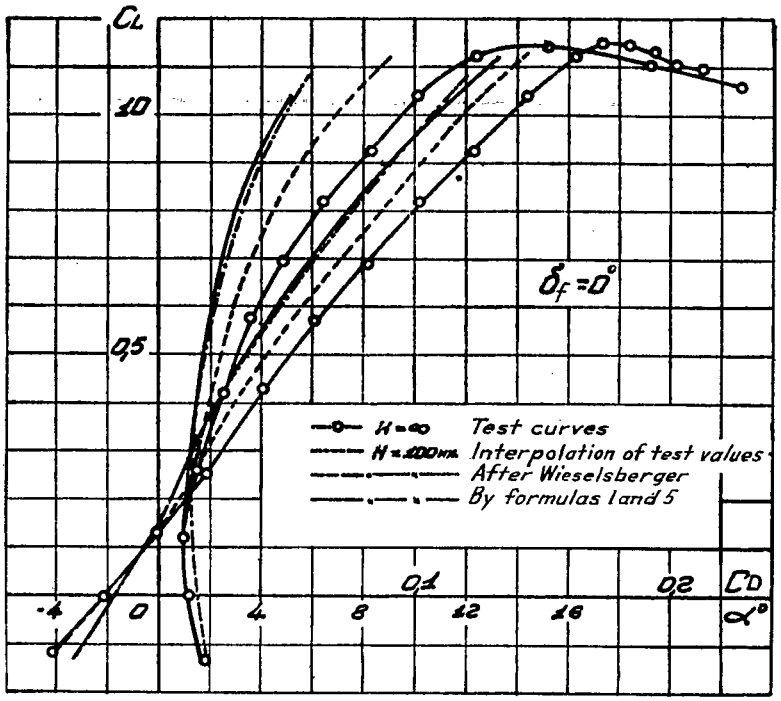
C_L
1.0
0.5
$\delta_f = 0°$
H = ∞ Test curves
H = 100 mm Interpolation of test values
After Wieselsberger
By formulas 1 and 5
0.1
0.2
C_D
-4
0
4
8
12
16
$\alpha°$

Fig. 30

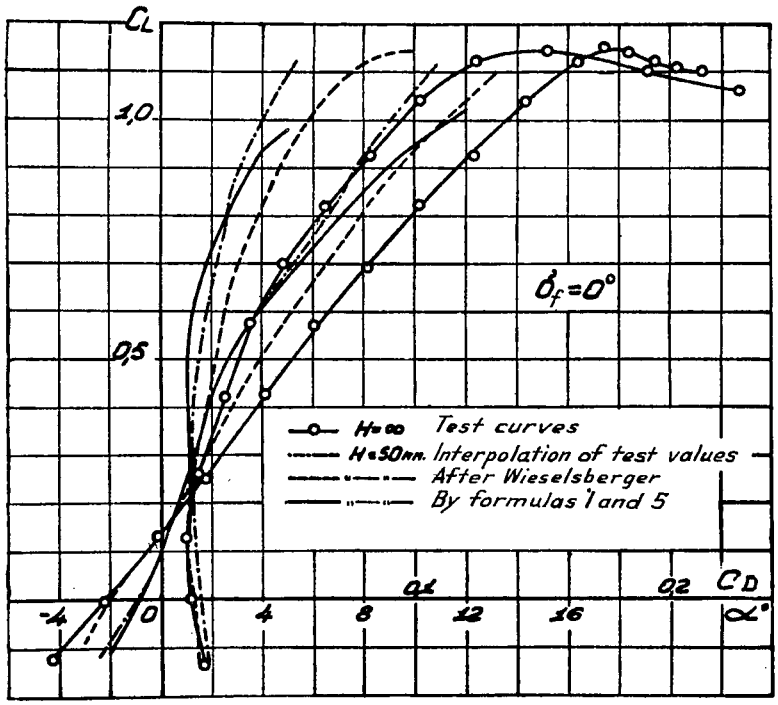
C_L
1.0
0.5
$\delta_f = 0°$
H = ∞ Test curves
H = 50 mm Interpolation of test values
After Wieselsberger
By formulas 1 and 5
0.1
0.2
C_D
-4
0
4
8
12
16
$\alpha°$

Fig. 31